

# Early twentieth-century warming linked to tropical Pacific wind strength

Diane M. Thompson<sup>1\*</sup>†, Julia E. Cole<sup>1,2</sup>, Glen T. Shen<sup>3</sup>, Alexander W. Tudhope<sup>4</sup> and Gerald A. Meehl<sup>5</sup>

**Of the rise in global atmospheric temperature over the past century, nearly 30% occurred between 1910 and 1940 when anthropogenic forcings were relatively weak<sup>1</sup>. This early warming has been attributed to internal factors, such as natural climate variability in the Atlantic region, and external factors, such as solar variability and greenhouse gas emissions. However, the warming is too large to be explained by external factors alone and it precedes Atlantic warming by over a decade. For the late twentieth century, observations and climate model simulations suggest that Pacific trade winds can modulate global temperatures<sup>2–7</sup>, but instrumental data are scarce in the early twentieth century. Here we present a westerly wind reconstruction (1894–1982) from seasonally resolved measurements of Mn/Ca ratios in a western Pacific coral that tracks interannual to multidecadal Pacific climate variability. We then reconstruct central Pacific temperatures using Sr/Ca ratios in a coral from Jarvis Island, and find that weak trade winds and warm temperatures coincide with rapid global warming from 1910 to 1940. In contrast, winds are stronger and temperatures cooler between 1940 and 1970, when global temperature rise slowed down. We suggest that variations in Pacific wind strength at decadal timescales significantly influence the rate of surface air temperature change.**

The recent slowdown of global atmospheric warming<sup>2</sup> probably reflects increased storage of heat in the ocean, and several regions may play important roles<sup>3,8</sup>. A strengthening of Pacific trade winds since the 1990s<sup>4,5</sup> as part of a larger shift to a negative phase of the Interdecadal Pacific Oscillation (IPO) has probably contributed to the slowdown<sup>3,6</sup>, and model studies demonstrate physically plausible mechanisms by which Pacific zonal wind variability can influence the rate of global temperature change<sup>3,4,6,7</sup>.

Between 1910 and 1940, global temperature warmed by 0.4 °C (Fig. 1) under an increase in anthropogenic forcing of only 0.3 W m<sup>-2</sup>, compared with 0.75 °C of warming under a 1.5 W m<sup>-2</sup> increase since 1970 (refs 1,9,10; Fig. 1). Detection/attribution studies with three generations of global coupled climate models have indicated that at least some of this early century warming was probably due to natural factors, such as very few volcanic eruptions and an increase in solar output<sup>10–12</sup> (Fig. 1). However, the magnitude of observed warming is greater than that simulated by climate models with forcing from external sources alone (0.20–0.25 °C; ref. 10), suggesting that internal variability played an important role in the early twentieth-century warming.

Although previous work has linked Atlantic warming to the rise in global atmospheric temperature<sup>13</sup>, Atlantic sea surface

temperatures (SSTs) were actually below average until the mid-1920s. The importance of internally generated climate variability in the Pacific region in recent decades<sup>6</sup> leads to the question of whether tropical Pacific variability contributed significantly to the early century warming. However, the lack of reliable wind and

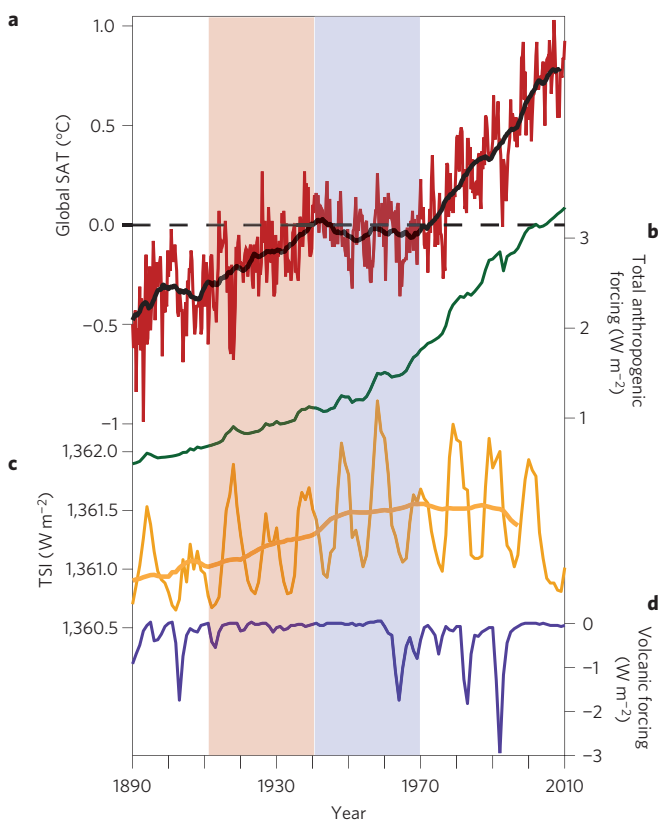


**Figure 1 | Comparison of global temperature with external forcings over the twentieth century. a**, Global surface air temperature (SAT) anomaly<sup>9</sup>, monthly (red) and 10-year smoothed (black). The record mean is indicated by the black dashed line. **b**, Total anthropogenic effective radiative forcing (W m<sup>-2</sup>; ref. 1). **c**, Total solar irradiance (TSI), annual and smoothed at 31 years (thick line; W m<sup>-2</sup>; ref. 1). **d**, Volcanic effective radiative forcing (W m<sup>-2</sup>; ref. 1). Shaded intervals denote periods of more rapid warming (1910–1940; red) and slower warming (1940–1970; blue) discussed in the text.

<sup>1</sup>Department of Geosciences, University of Arizona, Tucson, Arizona 85721, USA. <sup>2</sup>Department of Atmospheric Sciences, University of Arizona, Tucson, Arizona 85721, USA. <sup>3</sup>Proposal Exponent, Seattle, Washington 98177, USA. <sup>4</sup>School of GeoSciences, University of Edinburgh, Edinburgh EH9 3JW, UK. <sup>5</sup>Climate & Global Dynamics Division, National Center for Atmospheric Research, Boulder, Colorado 80307, USA. †Present address: National Center for Atmospheric Research, PO Box 3000, Boulder, Colorado 80307, USA. \*e-mail: thompsod@ucar.edu

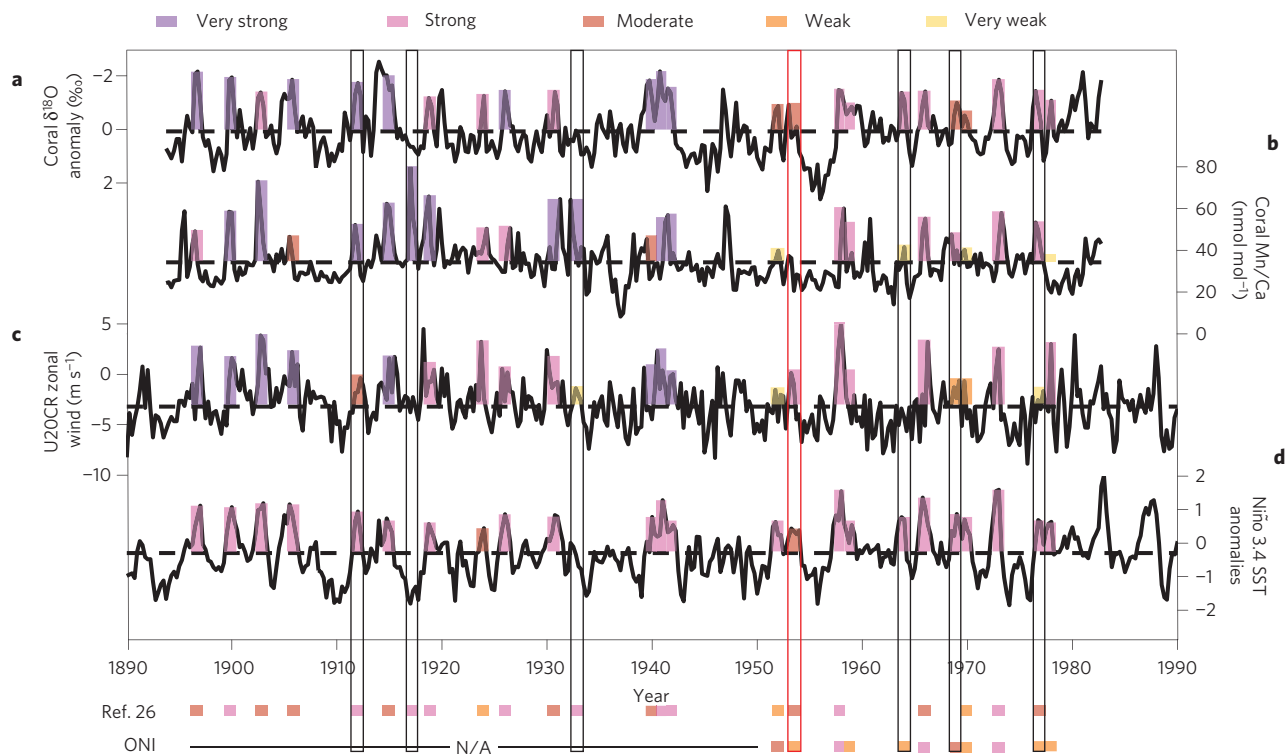


**Figure 2 | Comparison of coral Mn/Ca with indicators of Pacific climate over the twentieth century. a–d,** Quarterly detrended  $\delta^{18}\text{O}$  anomalies<sup>22</sup> (a) and Mn/Ca (b) from Tarawa Atoll, 20CR zonal wind in a  $10 \times 10$  degree gridbox surrounding Tarawa ( $4^\circ \text{S}$ – $6^\circ \text{N}$ ,  $166^\circ$ – $176^\circ \text{E}$ ; ref. 21; c) and Niño 3.4 SST index<sup>23</sup> (d), where shading denotes the strength of historical El Niño events in each data set<sup>26,27</sup> (bottom; see Methods and Supplementary Table 1). We highlight (black outline) events that are captured by the Mn/Ca data set, but are underestimated in the 20CR zonal wind data set. In contrast, only one event was absent from the Mn/Ca data set (red outline). ONI, Oceanic Niño index.

SST observations before about 1950 over most of the tropical Pacific<sup>5,14</sup> (Supplementary Fig. 1) makes it difficult to determine whether Pacific trade-wind variability influenced past rates of global temperature change.

The region near the Date Line and the Equator is particularly crucial for monitoring the effects of trade-wind strength on tropical Pacific SSTs and subsurface heat storage<sup>4</sup>. Yet, there are virtually no observations of early twentieth-century winds in this region (Supplementary Figs 1 and 2). Consistent with previous work<sup>14</sup>, we find considerable disagreement among wind products regarding the magnitude and sign of trade-wind variability over the twentieth century in this region (Supplementary Fig. 2). The lack of observations and the discrepancies among historical wind data sets highlight the need for an independent method to assess changes in zonal winds.

The skeletal Mn/Ca ratio in corals from atolls with west-facing lagoons offers a proxy for westerly wind anomalies<sup>15</sup>. Previous work has shown that at Tarawa Atoll<sup>15</sup>, situated near the Date Line and the Equator ( $1.33^\circ \text{N}$ ,  $172.97^\circ \text{E}$ ), coral skeletal Mn/Ca is high during El Niño events when zonal winds in the tropical Pacific are weak; Mn/Ca peaks also coincide with coral  $\delta^{18}\text{O}$  minima, reflecting warm and wet El Niño conditions. Westerly winds trigger strong physical mixing and release of Mn from the reducing environment of the lagoonal sediments, which are enriched in Mn relative to the overlying water column by 3 orders of magnitude as a result of the diagenetic reduction of  $\text{Mn}^{4+}$  to the more soluble  $\text{Mn}^{2+}$  species<sup>15</sup>. As a result, wind-driven mixing of only 1.3 cm of sediment would double the dissolved Mn concentration of the lagoonal sea water from 1 to 2 nM (ref. 15). Following wind-driven mixing events, Mn-enriched sea water is transported to the nearby fore-reef and incorporated in coral skeletons (Supplementary Fig. 3).

Other studies have suggested that coral Mn/Ca may reflect volcanic or terrigenous sources, or upwelling or advection of waters with anomalous Mn concentrations<sup>16–18</sup>. However, these factors are unlikely to be important at this small, remote equatorial atoll<sup>15</sup> (see Supplementary Discussion). Further, although a reduction in equatorial upwelling may contribute to anomalously high Mn/Ca during El Niño events, upwelling variations are small at this site and cannot account for the observed variability in skeletal Mn/Ca (Supplementary Discussion).

At this site near the Equator and the Date Line, westerly wind events are strongly tied to the state of both the interdecadal (IPO) and the interannual (El Niño/Southern Oscillation, ENSO) modes of variability within the basin (Supplementary Fig. 4). Westerly winds typically occur before and during El Niño events, when the sea level pressure gradient and trade winds are weak and the warm pool is extended eastward<sup>19</sup>. Strong (but short-term) westerly wind bursts initiate downwelling Kelvin waves that propagate eastward and participate in the onset and maintenance of El Niño events<sup>20</sup>. The resolution of the coral records and mixing time of lagoonal waters onto the reef precludes the ability to reconstruct individual wind burst events that occur over a few days. Nonetheless, elevated seawater Mn concentration resulting from westerly winds before and during El Niño events are captured in the Tarawa coral Mn/Ca record<sup>15</sup>. As westerly wind events are tied to the mean trade-wind strength<sup>19,20</sup>, which has been linked to recent variations in the rate of global warming<sup>4</sup>, reconstructed changes in westerly winds from Tarawa may provide insight into the role of Pacific winds in past warming variations.

Here we present a quarterly Mn/Ca record spanning 1894–1982 from a Tarawa *Porites* sp. coral (Methods) and compare it with ensemble mean zonal winds from the twentieth-century reanalysis

(20CR; Fig. 2)<sup>21</sup>. Coral Mn/Ca ranges from 8.3 to 80.2 nmol mol<sup>-1</sup>, with an average of  $34.2 \pm 10.2$  nmol mol<sup>-1</sup> and peaks associated with westerly winds and warm, wet conditions (negative  $\delta^{18}\text{O}$  anomalies<sup>22</sup>) during the major El Niño events of the twentieth century. Quarterly and annual (April–March) Mn/Ca correlate significantly with Tarawa coral  $\delta^{18}\text{O}$  (ref. 22), local zonal wind anomalies from the 20CR (ref. 21), and Niño 3.4 SST anomalies<sup>23</sup>, despite the fact that Mn/Ca tracks only the warm phase of ENSO (annual $\delta^{18}\text{O}$ :  $r_s = -0.42$ ,  $N = 88$ ,  $P < 0.001$ ; annual<sub>20CR</sub>:  $r_s = 0.43$ ,  $N = 88$ ,  $P < 0.001$ ; annual<sub>Niño3.4SSTa</sub>:  $r_s = 0.27$ ,  $N = 88$ ,  $P = 0.013$ ). The lower correlation between Mn/Ca and Niño 3.4 SST reflects the fact that the impact of westerly winds on tropical Pacific SSTs depends on the background state<sup>24,25</sup>. We also find a strong event-by-event correspondence in the amplitude of Mn/Ca, zonal wind,  $\delta^{18}\text{O}$  and Niño 3.4 SST during major historical El Niño events<sup>26,27</sup>, with the Tarawa Mn/Ca record capturing several strong well-documented El Niños<sup>26,27</sup> that are underestimated or absent in the 20CR zonal wind data set (Fig. 2 and Supplementary Table 1 and Discussion). The Mn/Ca from our new record also closely matches that published previously<sup>15</sup> from a *Hydnophora microconos* coral at Tarawa, and the Mn/Ca peaks of both records coincide (within age model uncertainties) with trade-wind reversals (Supplementary Fig. 5).

The Tarawa Mn/Ca record exhibits interdecadal modulation in the frequency of westerly winds (Supplementary Fig. 6) that corresponds with the rate of global atmospheric warming (Fig. 3). Mn/Ca pulses are more frequent during decades of rapid global warming and less frequent during slowly warming decades. This result is consistent with local weather station data for recent decades: more frequent westerly winds occurred at Tarawa during the accelerated warming interval of 1985–2000, and strong easterly winds characterized the current period of slower warming (2000–2009; Supplementary Fig. 7).

Just as stronger easterly trade winds seem to be important in the current warming slowdown, frequent westerly winds between 1910 and 1940 in our reconstruction suggests that weaker trade winds played a role in early twentieth-century accelerated warming (Fig. 3). Previously, internal variability in the Atlantic has been invoked to help explain this warming<sup>13</sup>, but Atlantic temperatures remain below average until the mid-1920s, over a decade after the onset of accelerated global warming. Our coral Mn/Ca reconstruction, in contrast, shows frequent westerly winds (weaker trade winds) as early as 1911, concurrent with the acceleration of warming. Anthropogenic forcing was non-negligible during this time and probably contributed to warming<sup>1</sup> (Fig. 1). Increased solar output may have played a role in this accelerated warming as well<sup>1</sup>, although the small rise in irradiance persisted from the start of the twentieth century to the 1950s (Fig. 1), whereas the warming rate levelled off between 1940 and 1970. Similarly, a lack of strong volcanic eruptions between 1905 and 1961 may have contributed, but does not overlap uniquely with the warming interval. Our data support a previously unrecognized role for internally generated Pacific trade-wind variability in contributing to the early twentieth-century warming, particularly before the mid-1920s.

The subsequent slowdown in warming between 1940 and 1970 coincides with stronger than average Pacific trade winds, little trend in solar output, and (in 1957) a sudden drop in North Atlantic SST (Figs 1 and 3). Anthropogenic influence was also intensifying through this interval (Fig. 1), with negative forcing from aerosols probably playing an important part in the slowdown<sup>1,10</sup>. Our Pacific trade-wind reconstruction supports a role for stronger Pacific trade winds as part of the mix of internal/external, natural/anthropogenic forcing that contributed to this slowdown in global atmospheric warming in the mid-twentieth century.

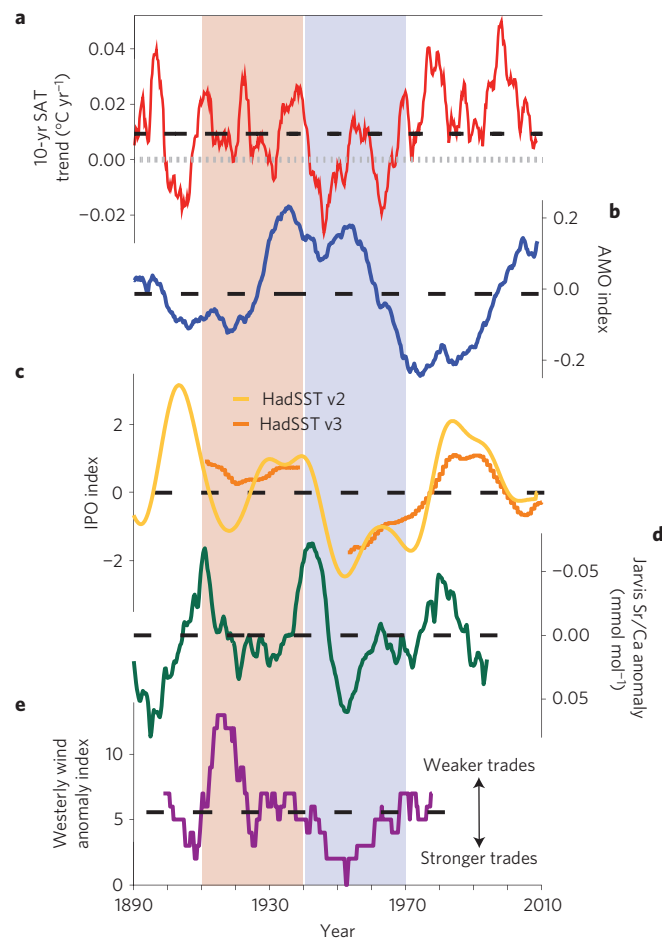


**Figure 3 | Comparison of the rate of global warming with internal variability over the twentieth century.** **a**, Ten-year linear trend in SAT (ref. 9). **b**, 11-year smoothed Atlantic Multidecadal Oscillation (AMO) index (from detrended HadSST v 3.1.0.0 data; <http://climexp.knmi.nl>). **c**, 11-year smoothed IPO index (from HadSST v2 (ref. 28) and HadSST v3). **d**, Ten-year smoothed coral Sr/Ca from Jarvis Atoll (warm SST plotted upwards). **e**, Tarawa coral westerly wind index (10-year sum of quarterly Mn/Ca with a Z-score  $\geq 1$ , that is,  $\geq 85$ th percentile). The black dashed lines denote the record means, and shading denotes the intervals discussed in the text (as in Fig. 1).

Decadal variability associated with the IPO corresponds with these intervals of accelerated and reduced global warming<sup>4,6</sup> (Fig. 3). Available SST observations (from the uninterpolated HadSST v3 data set, Fig. 3) suggest that the eastern Pacific was warmer than average during the early twentieth-century accelerated warming period, consistent with a new reconstruction of SST based on coral Sr/Ca from east of the Date Line (Fig. 3, see Methods). Although the IPO index based on earlier versions of the instrumental data set (for example, HadSST v2; ref. 28) suggests a negative state between  $\sim 1912$  and 1924 (Fig. 3), virtually no tropical observations are available for this period (Supplementary Fig. 1). Considered together, the available proxy-based reconstructions suggest that the tropical Pacific was significantly warmer between 1910 and 1940 than both the record mean and the 1941–1970 mean, consistent with weaker trade winds, frequent westerly winds near the Date Line, and accelerated warming between 1910 and 1940 (Supplementary Discussion). In contrast, there was no significant difference in Atlantic temperatures between these periods according to the available reconstructions of Atlantic multidecadal variability (Supplementary Discussion).



An important result of this study is to demonstrate that coral Mn/Ca can extend and improve the history of westerly wind events and trade-wind strength in the tropical Pacific. The coral Mn/Ca data from Tarawa adds to the twentieth-century climate record, revealing westerly winds during historic ENSO events that are not captured in the 20CR wind record. Extending this approach to present, and to other islands, would add to our understanding of the proxy–climate relationship and enable reconstruction of past changes in the broader Pacific wind field.

Our results support a strong connection between tropical Pacific westerly winds and the rate of global temperature rise, even during the early–mid twentieth century when anthropogenic forcing was smaller than today. We highlight the more frequent occurrence of equatorial westerlies during the period of rapid warming in the early twentieth century (1910–1940), which suggests that unusually weak Pacific trade winds are linked to past periods of accelerated warming. The importance of this mechanism, together with our understanding of Pacific decadal variability, suggests that global warming will accelerate when Pacific trade winds weaken and tropical Pacific SSTs shift yet again to a warmer state.

## Methods

Cores from a massive *Porites* sp. colony were collected in 1989–1990 on the southwest seaward fringe of Tarawa Atoll (Supplementary Fig. 3). A monthly  $\delta^{18}\text{O}$  record from this material correlates strongly with rainfall, SST and large-scale ENSO indices<sup>22</sup>. The current study uses the core material and age model from that earlier work, resampled at approximately quarterly (4 per year) increments using a miniature band saw. Quarterly resolution is used to detect trace concentrations of Mn incorporated in the coral skeleton (lattice-bound Mn in the carbonate matrix), but the accuracy of this sampling method may result in some variability in the temporal coverage of the Mn/Ca data between years. Mn/Ca analyses were produced on a graphite furnace atomic absorption spectrophotometer<sup>15,16</sup> ( $1\sigma$ :  $\pm 1.6$ – $2$  nmol Mn mol<sup>-1</sup> Ca) after rigorous cleaning in peroxide, reducing media, and acid following the methods of ref. 16.

The coral Sr/Ca record was developed from a core collected from a 4-m-diameter, massive *Porites* sp. coral at Jarvis Island (0° 22.3' S, 159° 59.0' W) in September 1999. The coral lived in an unrestricted setting, well flushed with open-ocean water, and the top of the coral was at 4 m water depth. Coral powders were drilled every 1 mm along optimal sampling transects parallel to the growth direction of individual corallites, and the chronology for the core was developed using X-ray images of the annual growth bands and identification of the seasonal cycle and major historical El Niño events in  $\delta^{13}\text{C}$ ,  $\delta^{18}\text{O}$ , and Sr/Ca. Scanning electron microscope images of samples from the top and bottom of the core were used to screen for the presence of alteration or diagenesis of the coral material. The coral samples were acidified in 2 ml of 5% trace metal grade HNO<sub>3</sub> and the ratio of strontium (407.77 nm) to calcium (393.37 nm) was measured every 2 mm of core on a JY Optima 2C inductively coupled plasma atomic emission spectrometer<sup>29</sup>. The long-term analytical precision ( $1\sigma$ ) was 0.0305 mmol mol<sup>-1</sup> for high-purity standards (0.33% RSD) and 0.044 mmol mol<sup>-1</sup> for an in-house coral standard (0.49% RSD). The strong correlation between SST and Sr/Ca measured in the Jarvis core over the period of overlap supports the interpretation of this Sr/Ca record in terms of local SST variability ( $r_s$  ranges between 0.42 and 0.67 for multiple SST data sets at monthly resolution). (The Jarvis Sr/Ca and Tarawa Mn/Ca records developed in this work can be accessed on the National Climate Data Center's Paleoclimatology database; <http://ncdc.noaa.gov/data-access/paleoclimatology-data>).

We compare this new Mn/Ca record with the Tarawa coral  $\delta^{18}\text{O}^{22}$  and the *H. microconos* Mn/Ca<sup>15</sup> records ([http://hurricane.ncdc.noaa.gov/pls/paleox/f?p=519:1:0:::P1\\_study\\_id:1845](http://hurricane.ncdc.noaa.gov/pls/paleox/f?p=519:1:0:::P1_study_id:1845)), 20CR zonal wind data<sup>21</sup> (which offers an improvement over previous products such as COADS data that are very patchy; [http://esrl.noaa.gov/psd/data/20thC\\_Rean/](http://esrl.noaa.gov/psd/data/20thC_Rean/)), and the Niño 3.4 ENSO SST index<sup>23</sup> (<http://iridl.ldeo.columbia.edu/expert/SOURCES/NOAA/NCDC/ERSST/version3b/.anom/X/%28190%29%28240%29RANGE/Y/%285%29%285N%29RANGE/dods>) to assess the connection between coral Mn/Ca and El Niño events (each quarterly and annually averaged using the April–March 'tropical' year). We note that the observed decrease in the ensemble spread of 20CR over time had no observed effects on the magnitude of interannual zonal wind variability. To compare the event strength, we calculated Z-scores ( $Z = (X_i - \mu)/\sigma$ ) for each data set from the magnitude of the event ( $X_i$ ) and the mean ( $\mu$ ) and standard deviation ( $\sigma$ ) of the period of overlap (1893.75–1982.75), and ranked each event as follows: very weak events:  $Z = 0.5$ – $0.84$  (~70–80th percentile), weak events:  $Z = 0.85$ – $0.99$  (~80–85%), moderate events:  $Z = 1$ – $1.2$  (~85–90%), strong events:  $Z = 1.21$ – $1.6$  (~90–95%), and very strong events  $\geq 1.6$

( $\geq 95\%$ ). We use the frequency of seasonal Mn/Ca Z-scores greater than 1 (summed over running 10-year intervals) to compare with global temperature trends, which are similarly calculated on seasonal anomalies (relative to 1951–1980) over running 10-year intervals. Finally, we compare variability in westerly winds and bursts over the twentieth century inferred from Mn/Ca and the 6-hourly 20CR zonal wind data. Westerly winds were defined as any positive 20CR zonal wind values, and bursts were defined as westerly winds  $\geq 5$  m s<sup>-1</sup> that lasted for 2 days<sup>30</sup>.

Received 8 July 2014; accepted 12 November 2014;

published online 22 December 2014

## References

- Myhre, G. D. *et al.* in *Climate Change 2013: The Physical Science Basis* (eds Stocker, T. F. *et al.*) Ch. 8 (IPCC, Cambridge Univ. Press, 2013).
- Trenberth, K. E. & Fasullo, J. T. An apparent hiatus in global warming? *Earth's Future* **1**, 19–32 (2013).
- Meehl, G. A., Arblaster, J. M., Fasullo, J. T., Hu, A. & Trenberth, K. E. Model-based evidence of deep ocean heat uptake during surface temperature hiatus periods. *Nature Clim. Change* **1**, 360–364 (2011).
- England, M. H. *et al.* Recent intensification of wind-driven circulation in the Pacific and the ongoing warming hiatus. *Nature Clim. Change* **4**, 222–227 (2014).
- L'Heureux, M. L., Lee, S. & Lyon, B. Recent multidecadal strengthening of the Walker circulation across the tropical Pacific. *Nature Clim. Change* **3**, 571–576 (2013).
- Meehl, G. A., Hu, A., Arblaster, J. M., Fasullo, J. & Trenberth, K. E. Externally forced and internally generated decadal climate variability associated with the Interdecadal Pacific Oscillation. *J. Clim.* **26**, 7298–7310 (2013).
- Kosaka, Y. & Xie, S. P. Recent global-warming hiatus tied to equatorial Pacific surface cooling. *Nature* **501**, 403–407 (2013).
- Chen, X. & Tung, K. K. Varying planetary heat sink led to global-warming slowdown and acceleration. *Science* **345**, 897–903 (2014).
- Hansen, J., Ruedy, R., Sato, M. & Lo, K. Global surface temperature change. *Rev. Geophys.* **48**, RG4004 (2010).
- Bindoff, N. L. *et al.* in *Climate Change 2013: The Physical Science Basis* (eds Stocker, T. F. *et al.*) Ch. 10 (Cambridge Univ. Press, 2013).
- Mitchell, J. F. B. *et al.* in *Climate Change 2001: The Scientific Basis* (eds Houghton, J. T. *et al.*) Ch. 12 (IPCC, Cambridge Univ. Press, 2001).
- Hegerl, G. C. *et al.* in *Climate Change 2007: The Physical Science Basis* (eds Solomon, S. D. *et al.*) 663–745 (IPCC, Cambridge Univ. Press, 2007).
- Schlesinger, M. E. & Ramankutty, N. An oscillation in the global climate system of period 65–70 years. *Nature* **367**, 723–726 (1994).
- Wu, R. & Xie, S. P. On equatorial Pacific surface wind changes around 1977: NCEP–NCAR reanalysis versus COADS observations. *J. Clim.* **16**, 167–173 (2003).
- Shen, G. T., Linn, L. J., Campbell, T. M., Cole, J. E. & Fairbanks, R. G. A chemical indicator of trade wind reversal in corals from the western tropical Pacific. *J. Geophys. Res.* **97**, 12698–12697 (1992).
- Shen, G. T. & Boyle, E. A. Determination of lead, cadmium and other trace metals in annually-banded corals. *Chem. Geol.* **67**, 47–62 (1988).
- Shen, G. T. *et al.* Paleochemistry of manganese in corals from the Galapagos Islands. *Coral Reefs* **10**, 91–100 (1991).
- Inoue, M. *et al.* Evaluation of Mn and Fe in coral skeletons (*Porites* spp.) as proxies for sediment loading and reconstruction of 50 yrs of land use on Ishigaki Island, Japan. *Coral Reefs* **33**, 363–373 (2014).
- Yu, L., Weller, R. A. & Liu, W. T. Case analysis of a role of ENSO in regulating the generation of westerly wind bursts in the western equatorial Pacific. *J. Geophys. Res.* **108**, 2002JC001498 (2003).
- Veccchi, G. A. & Harrison, D. E. Tropical Pacific sea surface temperature anomalies, El Niño, and equatorial westerly wind events. *J. Clim.* **13**, 1814–1830 (2000).
- Compo, G. P. *et al.* The twentieth century reanalysis project. *Q. J. R. Meteorol. Soc.* **137**, 1–28 (2011).
- Cole, J. E., Fairbanks, R. G. & Shen, G. T. Recent variability in the Southern Oscillation: Isotopic results from a Tarawa Atoll coral. *Science* **260**, 1790–1793 (1993).
- Smith, T. M., Reynolds, R. W., Peterson, T. C. & Lawrimore, J. Improvements to NOAA's historical merged land–ocean surface temperature analysis (1880–2006). *J. Clim.* **21**, 2283–2296 (2008).
- Fedorov, A. V. The response of the coupled tropical ocean–atmosphere to westerly wind bursts. *Q. J. R. Meteorol. Soc.* **128**, 1–23 (2002).
- Harrison, D. E. & Chiodi, A. M. Pre- and post-1997/98 westerly wind events and equatorial Pacific cold tongue warming. *J. Clim.* **22**, 568–581 (2009).
- Quinn, W. H., Neal, V. T. & De Mayolo, S. E. A. El Niño occurrences over the past four and a half centuries. *J. Geophys. Res.* **92**, 14449–1446 (1987).

27. NOAA's *Oceanic Niño Index (ONI)* (NOAA Climate Prediction Center); <http://www.cpc.ncep.noaa.gov/data/indices/oni.ascii.txt>.
28. Parker, D. E. *et al.* Decadal to interdecadal climate variability and predictability and the background of climate change. *J. Geophys. Res.* **112**, D18115 (2007).
29. Schrag, D. P. Rapid analysis of high-precision Sr/Ca ratios in corals and other marine carbonates. *Paleoceanography* **14**, 97–102 (1999).
30. Harten, L. M. Synoptic settings of westerly wind bursts. *J. Geophys. Res.* **101**, 16997–17019 (1996).

### Acknowledgements

We thank M. Price, S. Hlohowskyj, S. Lemieux, C. Hollenbeck and S. Sanchez for support in producing Mn/Ca and Sr/Ca data sets, and S. Worley and J. Comeaux for aid in obtaining weather station data. We are grateful for discussions with J. Overpeck, J. L. Russell, W. Beck, P. DiNezio and C. Deser. This research was supported by the NOAA Climate Program Office (awards NA16RC0082 and NA08OAR4310682), the US NSF (awards OCE-9158496 and EaSM2-1243125), The University of Arizona Department of Geosciences, the Philanthropic Education Organization, UK NERC (Grant NER/GR3/12021), and the Regional and Global Climate Modeling Program of the

US-DOE Office of Biological & Environmental Research Cooperative Agreement (DE-FC02-97ER62402).

### Author contributions

This study was initially conceived by G.T.S. and J.E.C., and Tarawa Mn/Ca time series data were generated by G.T.S. D.M.T. compiled and analysed Mn/Ca calibration data, and performed quantitative and comparative data analyses. A.W.T. conceived the Jarvis study, with D.M.T., J.E.C. and A.W.T. contributing to sampling, Sr/Ca analysis and interpretation. D.M.T., G.A.M. and J.E.C. led the comparisons of instrumental and palaeodata. D.M.T. and J.E.C. wrote the manuscript, and all authors contributed to discussion, interpretation and editing of the manuscript.

### Additional information

Supplementary information is available in the [online version of the paper](#). Reprints and permissions information is available online at [www.nature.com/reprints](http://www.nature.com/reprints). Correspondence and requests for materials should be addressed to D.M.T.

### Competing financial interests

The authors declare no competing financial interests.